

Supporting Information

Discovery of Non-Lipogenic ABCA1 Inducing Compounds with Potential in Alzheimer's Disease and Type 2 Diabetes

Manel Ben Aissa^{1,2*}, Cutler Lewandowski¹, Kiira Ratia³, Sue Lee¹, Brian Layden⁴, Mary Jo LaDu⁵, & Gregory R.J. Thatcher^{6*}

¹Department of Pharmaceutical Sciences, College of Pharmacy, University of Illinois at Chicago (UIC), Chicago, IL; ²UICentre (Drug Discovery @ UIC), UIC; ³HTS Screening Facility, Research Resources Center, UIC; ⁴Department of Medicine, UIC; ⁵Department of Anatomy and Cell Biology, College of Medicine, UIC, USA; ⁶Department of Pharmacology & Toxicology, College of Pharmacy, University of Arizona, Tucson, AZ, USA

Table of Contents	Page
Fig. S1. Representative data from HTS of 10k compound ChemDiv libraries	S1
Fig. S2. Representative data from HTS hit validation, and cholesterol efflux data	S2
Fig. S3. Representative data of <i>in vitro</i> hit profiling via pathway-focused PCR arrays related to cholesterol metabolism, glucose homeostasis, and inflammation	S3
Fig. S4. Representative immunoblots of cellular ABCA1	S4
Fig. S5. Target ID for NLAs at various nuclear receptors	S5
Fig. S6. Chemical structures	S6
Fig. S7. Effects of F4 and T0 treatments on severity of HFD-induced hepatic steatosis	S7
Fig. S8. Schematic paradigms of F4 and T0 <i>in vivo</i> treatments	S8
Table S1. Descriptions of gene targets and primers used for qRT-PCR	S9
Supplemental Methods	
• Reagents	
• Lipid Analysis	
• Histology	
• HTS Libraries	
• Human Primary Astrocytes	
• Cytotoxicity Assays	
• LanthaScreen TR-FRET LXR-Coactivator Assays	
• Transcriptional reporter assays	
• Behavioral Assays	S10
References for Supplemental Methods	S11
Keywords and Abbreviations	

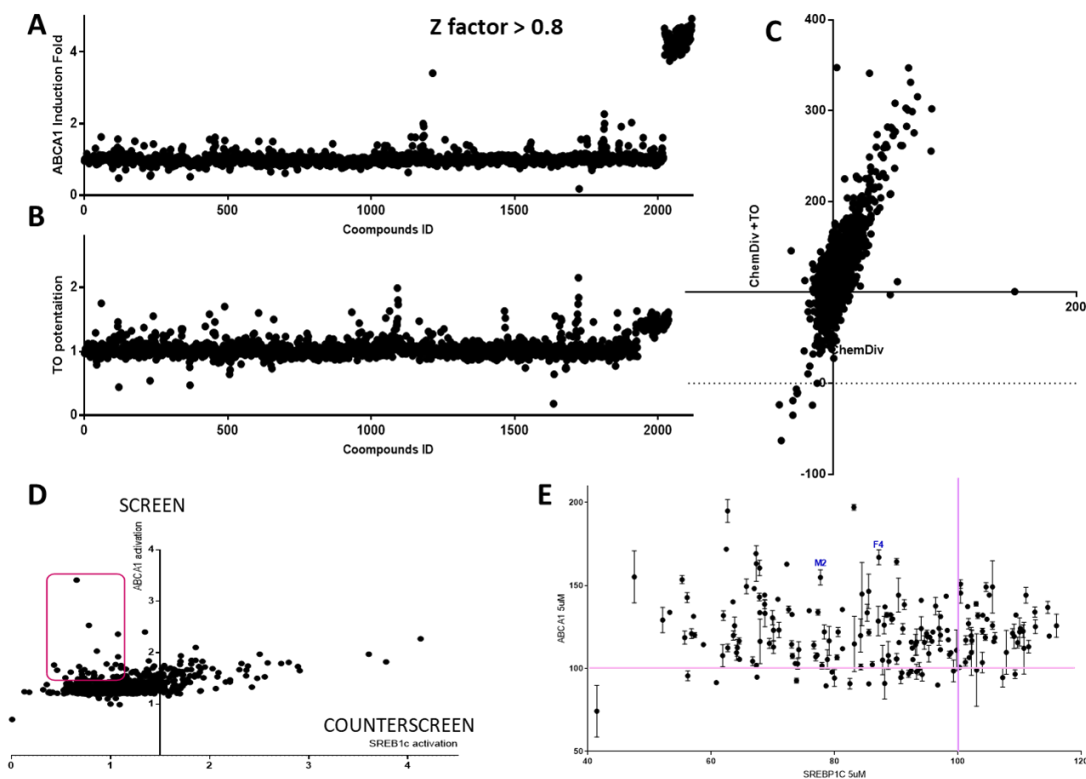


Fig. S1. Representative data from HTS of 10k compound ChemDiv libraries. **A)** ABCA1-luciferase induction in CCF-STTG astrocytoma cells was quantified, using LXR agonist T0901317 (T0) as positive control (Z' -factor > 0.6 in all experimental runs). **B)** ABCA1-luciferase induction was also measured in the presence of T0 (at $EC_{50} = 50$ nM) to identify hits that potentiated (or antagonized) T0 activity. **C)** Normalized screening data for ABCA1-luciferase induction in the presence (y-axis) and absence of T0 (x-axis) were correlated, relative to DMSO = 100%. **D)** ABCA1-luciferase fold-induction (y-axis) from primary screen was compared to SREBP1c-luciferase fold-induction (x-axis) in HepG2 cells from counterscreen, indicating that preferential activation of ABCA1 is possible. The desired selective activity of hits is shown (red box). **E)** Differential gene expression response was confirmed by repurchasing and rescreening actives for ABCA1- and SREBP1c-luciferase at 5 μ M. Hits F4 and M2 are indicated for reference.

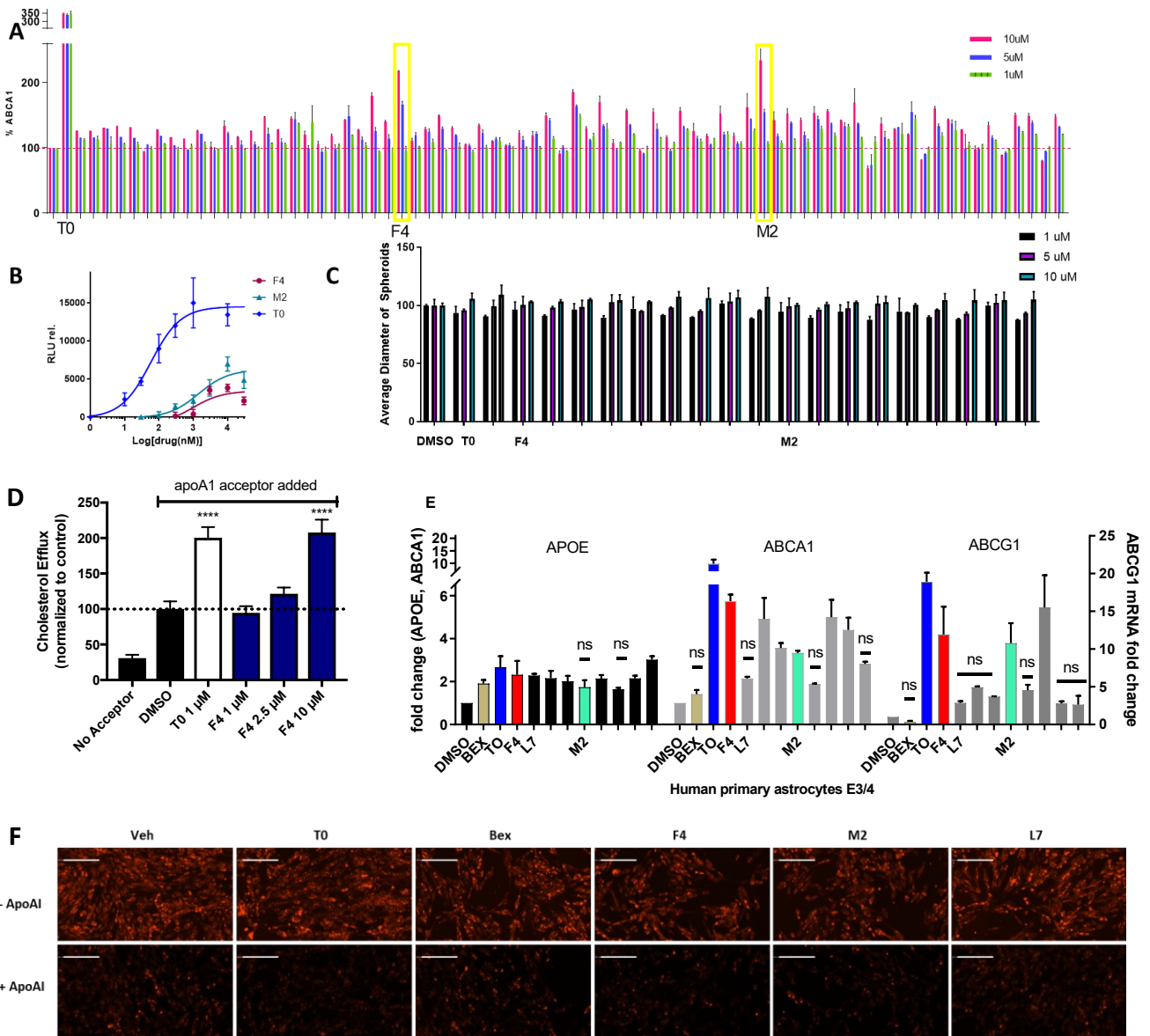


Fig. S2. Representative data from HTS hit validation. **A)** Concentration-response of ABCA1-luciferase induction normalized to DMSO control was used to selected hits for further screening in secondary assays (only hits F4 and M2 are annotated on the x-axis). **B)** Full concentration-response of ABCA1-luciferase for F4 and M2, compared to T0, was performed in HepG2 cells, although this assay was not optimized for use as a counterscreen. **C)** Cytotoxicity of test compounds was analyzed in 3D spheroid cultures of HepG2 cells, revealing no change in spheroid viability with F4 or M2. **D)** BODIPY-cholesterol efflux from J774 macrophages demonstrates efficacy of F4 similar to T0. **E)** ABCA1, ABCG1, and APOE mRNA levels measured by RT-PCR in primary human astrocytes after treatment with validated hits (labeled F4, L7, or M2 or unlabeled hits shown in grey) or benchmark agonists (all at 5μM), relative to DMSO vehicle control. All fold changes are significantly different from vehicle ($p < 0.05$) except those marked by ns. **F)** Representative images of BODIPY-cholesterol in CCF cells treated with T0, Bex, or hits, F4, M2, and L7, before and after addition of acceptor ApoA.

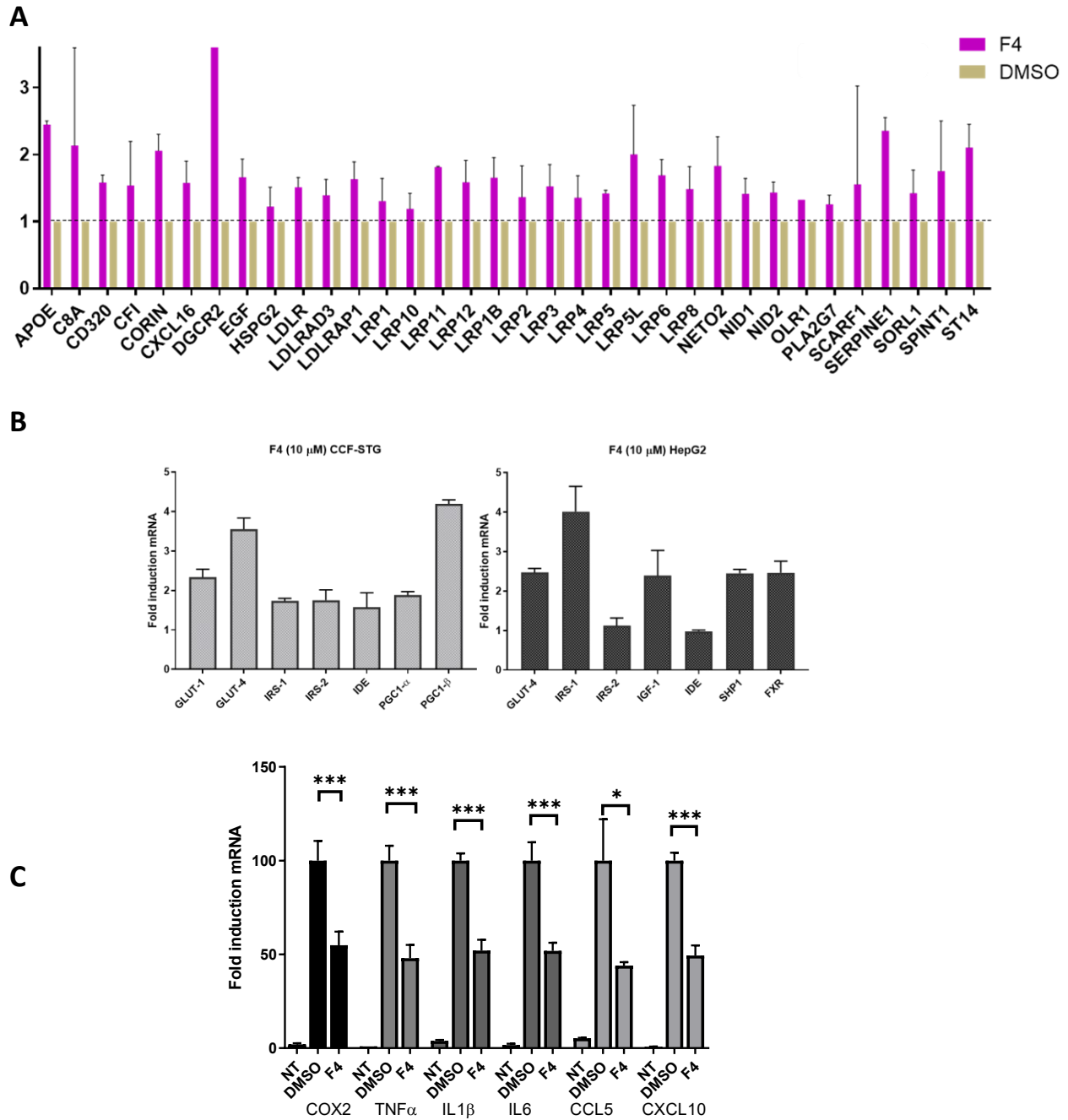


Fig. S3. Representative data of *in vitro* hit profiling via pathway-focused PCR arrays related to cholesterol metabolism, glucose homeostasis, and inflammation. A) Treatment with hit F4 (at 5 μ M) showed activation of LDL-related genes in HepG2 cells. **B)** Treatment with hit F4 (at 10 μ M) in CCF-STG1 (left) and HepG2 cells (right) indicated activation of genes involved in glucose metabolism. **C)** Treatment with 1 μ g/mL LPS in presence of DMSO vehicle control or hit F4 (at 10 μ M) in human primary astrocytes revealed reversal of LPS-induced proinflammatory marker gene expression by F4.

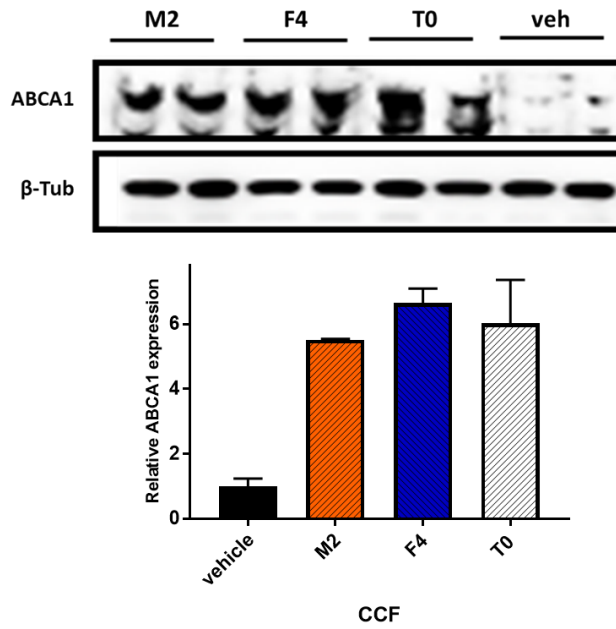
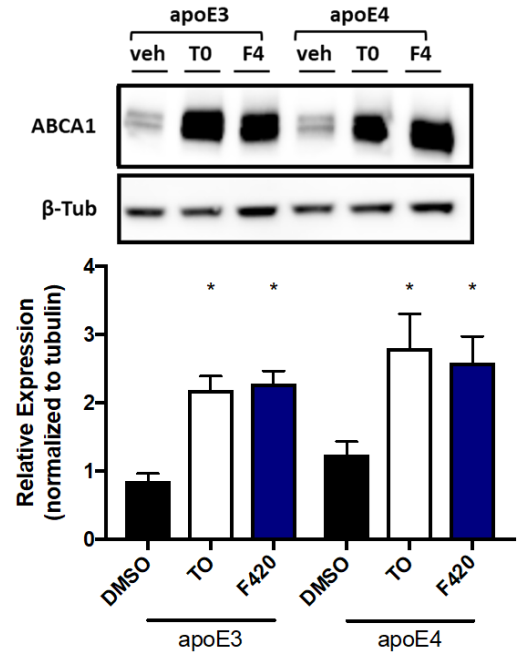
A**B**

Fig. S4. Representative Immunoblots of cellular ABCA1. **A)** CCF-STTG1 cells were treated with 5 μ M of T0, M2, F4 and control vehicle. **B)** Primary mouse astrocytes expressing *APOE3* and *APOE4* were treated with test compounds T0 or F4 at 5 μ M or vehicle.

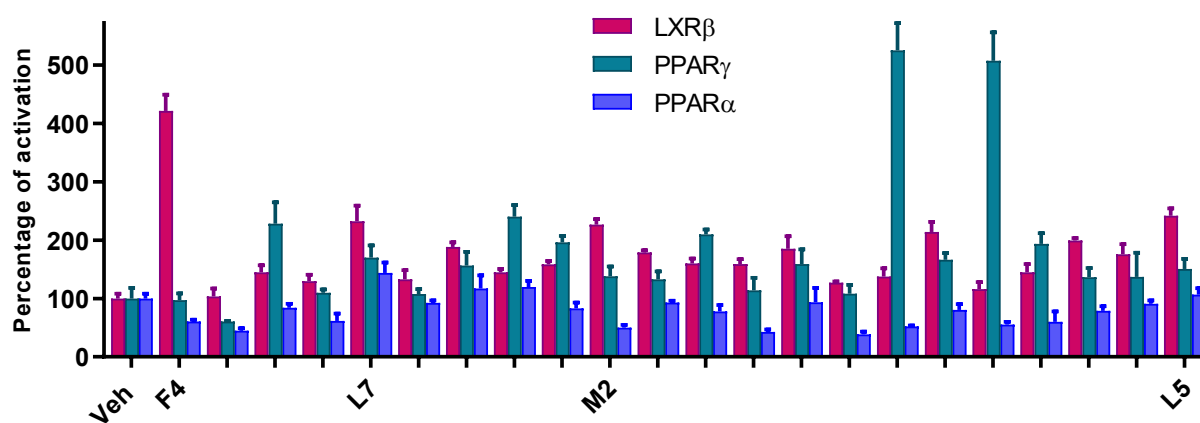


Fig. S5. Target ID for NLAI at various nuclear receptors. A) LXR β , PPAR γ and PPAR α transactivation by NLAI hits. F4 displayed significant LXR β agonistic activity (4.21 -fold) in luciferase reporter assay, while other NLAI displayed PPAR γ agonist activity. Only hits F4, M2, and L5 are labeled. All other validated hits that were tested represent are not labeled and are shown to demonstrate the diverse nuclear receptor profiles of hits NLAI.

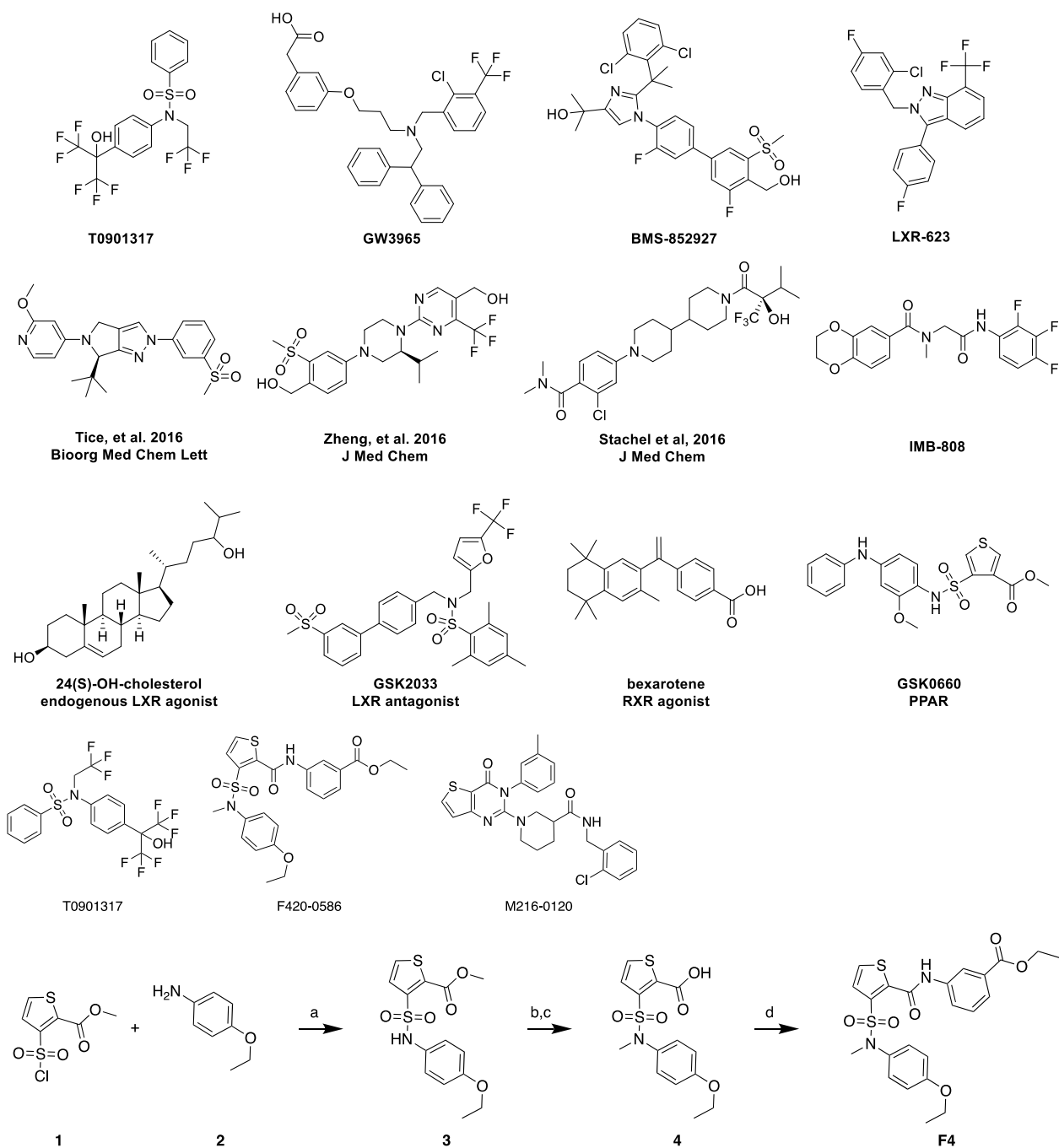
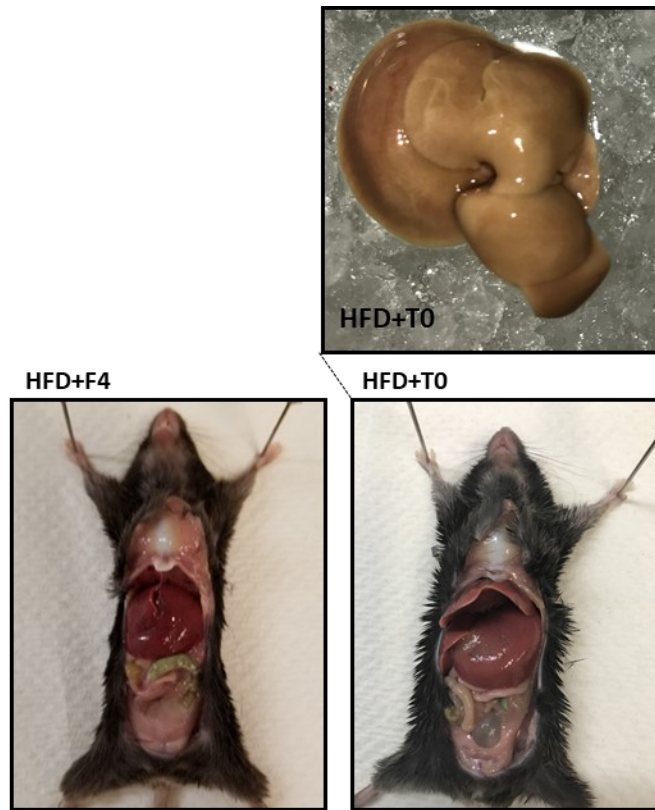


Fig. S6. Chemical structures. The structures of exemplar LXR agonists, positive control pan-LXR agonist T0901317 (T0) and hits F420-0856 (F4) and M216-0120 (M2). Synthetic scheme for F4: a) Et₃N, THF, 24h, rt. b) NaH/CH₃I, DMF, 24h, 0°C->rt. c) NaOH/H₂O, 24 h, rt. d) CO₂Cl₂/ethyl 3-amino benzoate, DCM, 24h, 40°C->rt.

A



B

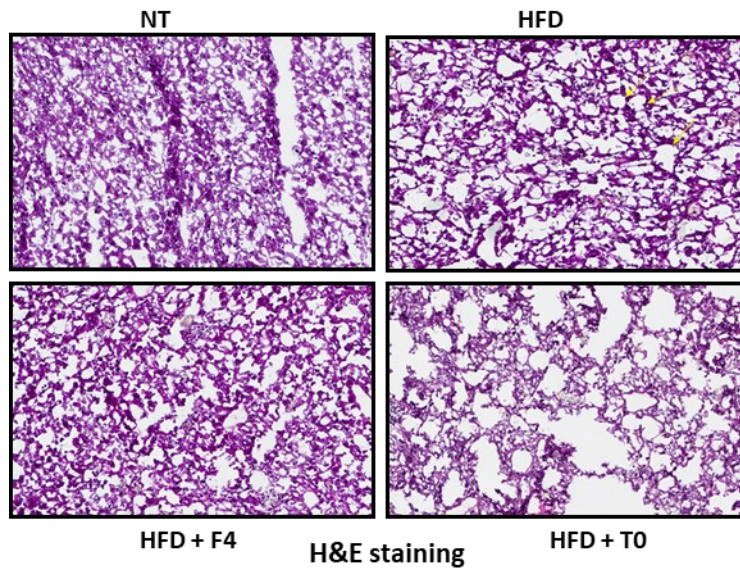


Fig. S7. Effects of F4 and T0 treatments on severity of HFD-induced hepatic steatosis. A) Gross morphology of livers from treated animals showing aggravation of HFD-induced fatty liver in T0-treated group, but not in F4-treated group. **B)** Liver morphology of H&E-stained sections from each mouse group after 8 wk of HFD and 4 weeks of experimental treatment showing aggravation of lipid aggregation in liver sections treated with T0.

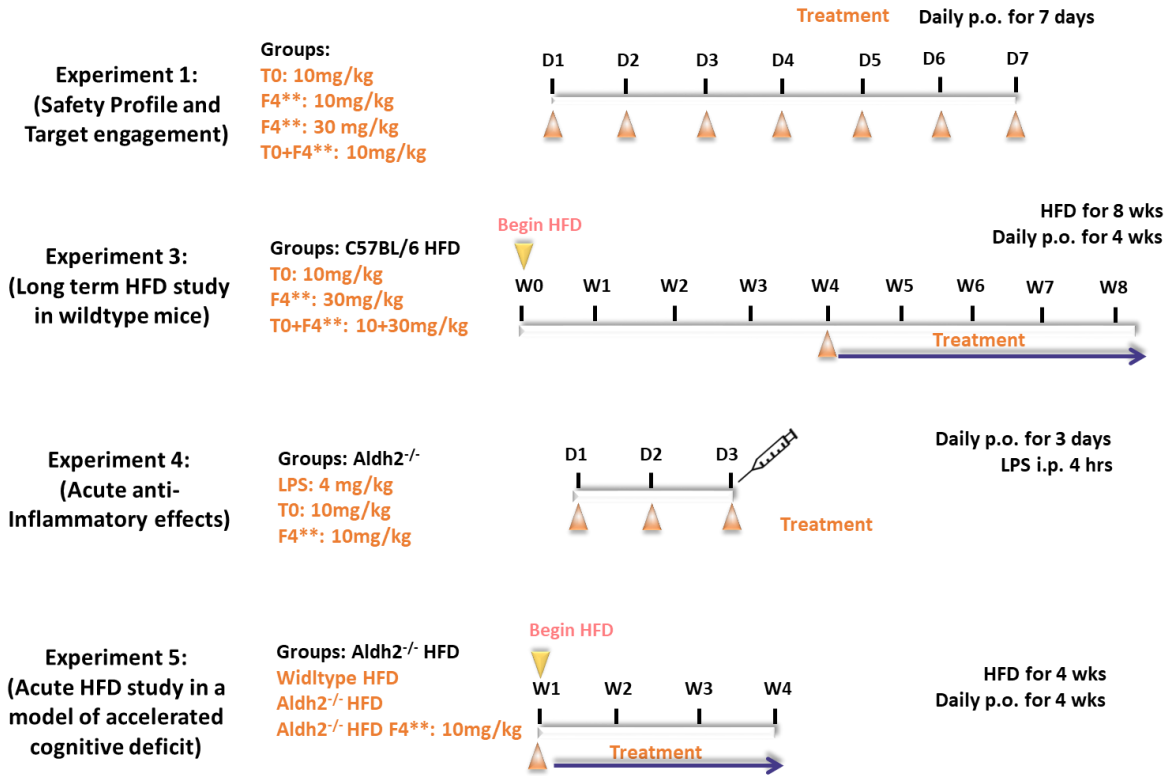


Fig. S8. Schematic paradigms of F4 and T0 *in vivo* treatments. A, mice were treated with F4 or T0 daily by gavage (p.o.) at 10mg/kg and 30mg/kg. For HFD studies, mice were fed high fat diet ad libitum with or without F4 and T0 for 4 or 8 weeks at 10 mg/kg and 30 mg/kg.

Name	Primer	Known function
<i>ABCA1</i>	Hs01059118_m1 (human) Mm00442646_m1 (mouse)	ATP-dependent cholesterol efflux
<i>ABCG1</i>	Hs00245154_m1 (human) Mm00437390_m1 (mouse)	ATP-dependent cholesterol efflux
<i>ACTB</i>	Hs99999903_m1 (human) Mm02619580_g1 (mouse)	Reference gene, encodes β -actin
<i>APOE</i>	Hs00171168_m1 (human) Mm01307193_g1 (mouse)	Plasma and CNS cholesterol transporter
<i>COX2</i>	Hs00153133_m1 (human) Mm03294838_g1 (mouse)	Pro-inflammatory enzyme, involved in prostaglandin synthesis
<i>CCL2</i>	Hs00234140_m1 (human) Mm00441241_m1 (mouse)	Pro-inflammatory chemokine
<i>CCL5</i>	Hs00982282_m1 (human) Mm01302427_m1 (mouse)	Pro-inflammatory chemokine
<i>CXCL10</i>	Hs00171042_m1 (human) Mm00445235_m1 (mouse)	Pro-inflammatory chemokine
<i>FASN</i>	Hs01005622_m1 (human) Mm00662319_m1 (mouse)	Fatty acid synthesis, encodes FAS
<i>HPRT</i>	Hs02800695_m1 (human) Mm03024075_m1 (mouse)	Reference gene, encodes hypoxanthine-guanine phosphoribosyltransferase
<i>IL1B</i>	Hs01555410_m1 (Human) Mm00434228_m1 (mouse)	Pro-inflammatory cytokine
<i>IL6</i>	Mm00446190_m1 (mouse) Hs00174131_m1 (human)	Pro-inflammatory cytokine
<i>NOS2</i>	Hs01075529_m1 (human) Mm00440502_m1 (mouse)	Pro-inflammatory enzyme, synthesizes nitric oxide
<i>PPARGC1</i>	Mm01208835_m1 (mouse) Hs00173304_m1 (Human)	mitochondrial biogenesis and metabolism, encodes PGC-1 α
<i>SCD1</i>	Hs01682761_m1 (Human) Mm00772290_m1 (mouse)	Fatty acid synthesis
<i>SIRT1</i>	Mm01168521_m1 (mouse)	Epigenetic regulator of stress- and longevity-related genes
<i>SCARB1</i>	Mm00450234_m1 (mouse)	Cellular cholesterol transport, encodes SR-BI
<i>SREBF1</i>	Hs01088691_m1 (human) Mm00550338_m1 (mouse)	Transcription factor controlling triglyceride synthetic genes, encodes SREBP1c
<i>TNF</i>	Hs00174128_m1 (Human) Mm00443258_m1 (mouse)	Pro-inflammatory cytokine, encodes TNF α

Table S1. Description of gene targets and primers used for qRT-PCR. Primers used as part of Taqman pathway-based qPCR arrays (**Fig. S3**) are not included here but are listed on manufacturer's website.

Supplemental Methods

Reagents. Commercially available agonists, including 22R-hydroxycholesterol (22R-HC), T0901317, GW3965, bexarotene, and LX100268 were purchased from Cayman Chemical Co. rApoA1 was purchased from Calbiochem. BODIPY-cholesterol was purchased from Invitrogen.

Lipid analysis. Triglyceride concentrations from each tissue type were determined via colorimetric assay, with tissue preparation and analysis performed according to the manufacturer's recommendations (Abcam ab65336). Similarly, HDL cholesterol (HDL-C), LDL cholesterol (LDL-C), and total cholesterol (TC) determination was performed using a fluorometric assay per the manufacturer's recommendations (Abcam ab65390).

BODIPY-cholesterol efflux in J774 macrophage cells. In serum-free media, J774 cells were loaded with 0.5 μ M BODIPY-chol (24h), then treated with compound (24h), then provided 20 μ g/mL purified apoA1 protein acceptor. After 6h, fluorescence (Ex/Em: 480/530) was separately measured in media and remaining cell lysate and quantified as % efflux = (media FL)/(media FL + cell FL), then normalized to DMSO = 100%.

Histology. Liver samples from HFD mice were fixed in 4% PFA, dehydrated, and embedded in paraffin. Serial 4- μ m sections were cut on sliding microtome (Leica RM2255 Microtome) and stained with hematoxylin and eosin (H&E) using standard procedures. Histological assessment was performed at the Research Histology and Tissue Imaging Core at UIC.

HTS libraries. The following libraries were used for the HTS campaign and are available within the UICentre for Drug Discovery, HTS Core Facility (Director: Gregory Thatcher): ChemDIV, a collection of 10,000 pharmacologically active compounds; Nuclear Receptors (200), spectrum collection; Prestwick Chemical Library, which includes 1,300 FDA-approved small molecules. The total number of screened compounds was 11,500. Test compound were first screened in CCF-ABCA1 at 10 μ M for ABCA1 activation with 1.5 fold activation compared to vehicle control as cutoff, then counterscreened at 5 and 10 μ M in HepG2-SREBP1c to ensure no SREBP1c activation. Hit validation was performed by concentration-response assay to determine EC50, using newly purchased compounds (purity > 98%) from different vendors (ChemDiv, Enamine, etc.) or from in-house scale-up synthesis.

Primary Astrocytes. Human Primary astrocytes isolated from human cortex were purchased (ScienCell). *APOE3/4* genotype donors were used. Each vial of cells, cryopreserved at passage one, can be used to 15 population doublings (up to five passages). Mouse primary astrocytes expressing human *APOE4/4* were directly isolated from E4FAD mice as previously described.¹ Selected hits were tested for secondary validation in mouse and human primary astrocytes expressing *APOE4/4* and *APOE3/4*, respectively. Following 24-hour treatment with 5 μ M test compound, mRNA levels of ABCA1, ABCG1 and APOE genes were determined using RT-PCR (see next section). Validated hits were further profiled in primary human astrocytes treated at 5 μ M with several RT-PCR arrays: TaqMan[®] Array Human LDL Pathways, TaqMan[®] Array Human Inflammation, TaqMan[®] Array Human Lipoprotein Signaling & Cholesterol Metabolism, TaqMan[®] Array Human ABC Transporters, TaqMan[®] Array Human Insulin Signaling Pathway, TaqMan[®] Array Human Glucose Metabolism, and TaqMan[®] Human Nuclear Receptor Array (96-well plate format, Thermofisher).

Cytotoxicity assays. Cytotoxicity was estimated for validated hits using MTT assay following standard protocol in two-dimensional HepG2 cell cultures and the CellTiter-Glo® 3D Cell Viability Assay (Promega) following manufacturer instructions in three-dimensional HepG2 spheroid cell culture.

LanthaScreen TR-FRET LXR-Coactivator Assays. LanthaScreen time-resolved fluorescence energy transfer (TR-FRET) LXR α -Coactivator Assay Kit (PV4655; ThermoFisher Scientific) and LXR β -Coactivator Assay Kit (PV4658; ThermoFisher Scientific) were used to determine binding and agonist activity at LXR α and LXR β , respectively. Test compounds were serially diluted from DMSO stocks in TR-FRET coactivator Assay buffer, and assays were run per the manufacturer's instructions. Briefly, increasing concentrations of test compound or control agonists (T0 and GW) were added to 384-well black plates (Costar). LXR α -LBD or LXR β -LBD protein was then added, followed by mixed coregulator and FL-peptide/Tb-anti-GST. The plates were gently shaken and incubated in darkness at room temperature for 2 hours, after which the 520/495 TR-FRET ratio was measured using the Synergy Neo2 Hybrid Multi-Mode plate reader (BioTek Synergy) using the following filter set: excitation 340 nm, emission 495 nm, and emission 520 nm. A 100 μ s delay followed by a 200 μ s integration time was used to collect the time-resolved signal. Results are displayed as percent activation compared to maximal activation of positive control (T0).

Transcriptional reporter assays. Validated Chinese Hamster Ovary (CHO) cell line-based human nuclear receptor luciferase reporter assay systems for LXR α , LXR β , PPAR α , and PPAR γ from Indigo Biosciences (State College, PA) were used for determination of the transactivation activity of test compounds. Equal volumes of reporter cells (100 μ l) were seeded into wells of opaque white 96-well tissue culture plates (Costar 3917). Cell media was replaced 16 h after plating with DMEM containing 10% stripped FBS and incubated for 24 h. Cells were then treated with test compounds at indicated concentrations in the figure captions. Matching vehicle (DMSO) and positive control agonists were included in each experiment. Twenty-four hours after treatment, cells were lysed with passive lysis buffer (Promega) according to the manufacturer's recommended procedures for 30 min. Luciferase activity was measured using the luciferase reporter assay kit (Promega) on the BioTek Synergy Neo2 Multimodal plate reader. The fold induction of luciferase activity was calculated relative to vehicle-treated cells and is the mean of three independent samples per treatment group.

Behavioral Testing. Novel object recognition (NOR) protocol was adapted from Leger, M. et al.² Briefly, mice were allowed to explore the empty test box for 5 min, returned to home cage, and allowed to explore the empty test box once more for 5 min (habituation phase). 24-hrs later, mice were subjected to the familiarization and testing phase. For the familiarization phase, two identical objects (small Lego towers) were placed in opposite corners of the test box. Mice were placed into the test box and allowed to freely explore for 10 min. For the testing phase, one original object (from the familiarization phase) and one novel object (plastic vial filled with bedding) were placed in opposite corners of the test box, maintaining location and orientation from the preceding familiarization phase. Mice were allowed to freely explore for 10 min or until the objects were explored for a total of 20 sec. The amount of time (sec) spent exploring was recorded for both the novel object and original object to calculate the discrimination index (DI% = $(\text{time}_{\text{novel object}} - \text{time}_{\text{familiar object}}) / \text{time}_{\text{total of exploration for both}}$).

References for Supplemental Methods

1. Fagan, A.M. *et al.* Unique lipoproteins secreted by primary astrocytes from wild type, apoE (-/-), and human apoE transgenic mice. *J Biol Chem* **274**, 30001-7 (1999).
2. Leger, M. *et al.* Object recognition test in mice. *Nat Protoc* **8**, 2531-7 (2013).

Keywords

ATP-Binding Cassette Transporter A1 (ABCA1); Cholesterol efflux; liver X receptor (LXR); peroxisome proliferator-activated receptor (PPAR); Lipogenesis; sterol receptor element binding protein 1C (SREBP1c); Anti-inflammation; high-fat diet (HFD)

Abbreviations

24S-OHC:	24-(S)-hydroxycholesterol
A β :	amyloid-beta
ABC:	<u>ABCA1-boosting compound</u>
ABCA1:	ATP binding cassette transporter A1
ABCG1:	ATP binding cassette transporter G1
ADRD:	Alzheimer's disease and related dementia
ALDH2:	aldehyde dehydrogenase 2
APOA1:	apolipoprotein A1
APOE:	apolipoprotein E
Bex:	RXR agonist bexarotene
CHO:	Chinese hamster ovary
CNS:	central nervous system
CRT:	coactivator recruitment TR-FRET
CSF:	cerebrospinal fluid
CVD:	cerebrovascular disease
DAM:	disease-associated microglia
EC ₅₀ :	half-maximal effective concentration (conc. at which 50% max. response occurs)
EFAD:	mouse model expressing five FAD mutations and human <i>APOE</i> alleles
E _{max} :	maximal efficacy
FAD-Tg:	familial AD transgenic mouse model
FAS:	fatty acid synthase
H&E:	hematoxylin and eosin
HDL-C:	high density lipoprotein cholesterol
HFD:	high-fat diet
HTS:	high-throughput screen
KO:	knockout
LAM:	lipid-droplet accumulating microglia
LDL-C:	low density lipoprotein cholesterol
LDLR:	low density lipoprotein receptor
LPS:	lipopolysaccharide
LRP-1:	LDLR-related protein 1

LXR:	liver X Receptor
LXRE:	LXR response element
NOR:	novel object recognition
NR:	nuclear receptor
PAINS:	pan-assay interference compounds
PGC-1 α :	PPAR γ coactivator 1 α
PPAR:	peroxisome proliferator-activated receptor
RCT:	reverse cholesterol transport
RXR:	retinoid X receptor
SCD:	stearoyl-CoA desaturase
SREBP:	sterol response element binding protein
STAT1:	signal transducer and activator of transcription 1
T0:	LXR agonist T0901317
T2D:	type 2 diabetes mellitus
TR-FRET:	time-resolved Förster resonance energy transfer
WT:	wild type